

## RESEARCH PAPER

# Biological Indicators Reveal Small-Scale Sea-Level Variability During MIS 5e (Sur, Sultanate of Oman)

M. Falkenroth<sup>\*†</sup>, S. Adolphs<sup>†</sup>, M. Cahnbley<sup>†</sup>, H. Bagci<sup>†</sup>, M. Kázmér<sup>‡,§</sup>, S. Mechernich<sup>||,¶</sup> and G. Hoffmann<sup>\*†</sup>

In this study we aim to document various coastal notches in Sur Lagoon (Oman) and interpret them regarding their use as sea-level indicator. We also unravel any short-term sea-level fluctuations, which are potentially preserved within the trace fossil assemblages of some of the notches. The oldest paleo notches stem from the last interglacial sea-level highstand of MIS 5e. This is concluded from cosmogenic nuclide dating of the fanglomerate bedrock in Sur Lagoon as presented in this study. All outcrops of paleo notches around Sur Lagoon were investigated in regards to the faunal distribution and notch shape. Furthermore, the absolute elevation of the notches and biological markers relative to msl were measured with a differential GPS.

The bioerosional notch occurs at the same height around Sur Lagoon indicating that the area remained tectonically stable over the last 125 kyr. According to the elevation of the notch-apex, msl was  $3.93 \pm 0.12$  m higher than today during the last interglacial. The distribution of boring and bioconstructing organisms relative to the notch shape displays at least one phase of short-term sea-level rise subsequent to the notch formation. The beachrocks that are associated with the bioerosion notches in Sur Lagoon show a larger grainsize than any sediment that is deposited in the lagoon nowadays. This, in combination with the occurrence of exceptionally high and deep abrasion notches, indicates that the coastline was more openly exposed and thus experienced a higher wave energy during the notch formation.

**Keywords:** bioerosion; tidal notch; last interglacial; sea-level; Oman; Indian Ocean

## 1 Introduction and aims

The understanding of natural processes along the world's coastlines is of socio-economic relevance as coastal areas host the largest share of the global population and a number of critical infrastructure. Processes that pose a potential threat to that infrastructure and population, such as short- or long-term sea-level rise, are naturally at the center of attention. Like every natural process, sea-level change is part of a complex system and understanding which parameters control it, is a challenging endeavor. This is especially true given that instrumentally recorded observations of the planet's climate systems only reach back a mere 200 years and many parameters like global mean temperature (IPCC, 2018) or the atmosphere's greenhouse-gas concentration are higher today than at

any other point in the last 800 kyr (Lüthi et al. 2008 and references therein). If we want to be able to assess future scenarios, proxy-based reconstructions of past climate systems, preferably of times as warm or warmer than today, are necessary. Past interglacials fit this requirement and are therefore of interest to the scientific community. For example during the last interglacial (128 to 116 kyr, marine isotope stage MIS 5e; Stirling et al. 1998) the greenhouse-gas concentration as well as summer insolation at high latitudes were slightly higher than pre-industrial levels (Petit et al. 1999), which caused 3°–5°C warmer polar temperatures (Otto-Bliesner et al. 2006) and a 1.5°C warmer global mean temperature (Abad et al. 2013; Lorscheid et al. 2017; Rohling et al. 2008; Shackleton et al. 2003) relative to today. The polar ice sheets were smaller (e.g. Kopp et al. 2009), the eustatic sea-level 6 m (+/–3 m) higher (Sisma-Ventura et al. 2017) and in some parts of the world, during short-term fluctuations, up to 10 m higher (Abad et al. 2013, Rohling et al. 2008). The number of sea-level peaks during the MIS 5e highstand is still uncertain (Abad et al. 2013). It is predicted that with rising global temperatures, initiated by anthropogenic greenhouse-gas emissions, the climatic conditions of the future will be similar to the conditions during MIS 5e (IPCC, 2013). In contrast to the situation today, orbital forcing on insolation instead of greenhouse-gas emission is seen as the main

\* NUG, RWTH Aachen University, DE

† Environmental Geology, Institute of Geoscience, University Bonn, DE

‡ Department of Palaeontology, Eötvös University, Budapest, HU

§ MTA-ELTE Geological, Geophysical and Space Science Research Group, Budapest, HU

|| Institute of Geology and Mineralogy, University of Cologne, DE

¶ Federal Institute of Hydrology, Koblenz, DE

Corresponding author: M. Falkenroth  
([michaela.falkenroth@rwth-aachen.de](mailto:michaela.falkenroth@rwth-aachen.de))

driver of the warming in MIS 5e (Hearty & Tormey 2017, Rohling et al. 2008, Rovere et al. 2016). Nevertheless, the response of coastal systems to a change in sea-level will be comparable, as they follow the same physical principles. Geomorphological indicators of former sea-level can be used to quantify sea-level variability. Suitable coastal landforms are for example marine terraces, benches or coastal notches (e.g. Abad et al. 2013, Hearty et al. 2007, Rovere et al. 2016). Our study area is a lagoon located on a poorly studied coastline of Oman. Around the lagoon a number of well-preserved coastal notches, reaching up to 3.93 m above msl, are observed. Dating results from previous studies (Mauz et al. 2015) and new results indicate a possible last interglacial age for the coastal notches, which will be discussed in this paper. However, the central goal of this study is to describe and document these coastal notches and to unravel any short-term sea-level fluctuations during a longer highstand that are preserved within the coastal notches in Sur. Furthermore, we add the investigated outcrops to the global database of interglacial coastlines, that is currently collected by the scientific community (pers. Comm. A. Rovere).

### 1.1 Coastal Notches

Coastal notches are horizontal incisions in cliffs with depths ranging from centimeters to meters. They form due to bioerosion, abrasion, chemical and physical weathering, or, most commonly, a combination of these processes (Rovere et al. 2016, Trenhaile 2015).

Among coastal notches, notches that contain trace fossils (referred to as bioerosion notches in the following) are known to enable sea-level reconstructions with the highest accuracy, because their biological zonation reflects the exact position of msl during their formation (e.g. Benac et al. 2004; Furlani et al. 2011; Rust & Kershaw, 2000). Bioerosion notches form preferably in microtidal seas (Evelpidou et al. 2012a) during periods of stable sea-level, which have to last for at least 0.10 ka (Abad et al. 2013; Pirazzoli 1986; Rovere et al. 2016; Sisma-Ventura et al. 2017). Besides bioerosional features the notch morphology, described through position of the deepest point of incision (apex) and the distance of notch roof and notch floor (notch width), can be related to sea-level during notch formation. The position of the apex can reflect the position of msl, but is also strongly influenced by wave exposure, while the width of the notch mirrors the total extent of the intertidal zone (Antonioli et al. 2015). Since the organisms inhabiting a coastal cliff react faster to sea-level changes than the notch-morphology, their vertical distribution in combination with a notch holds the potential to identify short-term sea-level variations within a period of a relatively stable highstand (Bromley & Asgaard 1993; Laborel & Laborel-Deguen 1994).

Notches that show no traces of bioerosion are harder to tie to a specific water depth or tidal datum, since their main process of formation is less obvious. While the absence of traces does not exclude bioerosion as a formation process, these notches can also form purely through wave action and originate at every point where waves or currents occur (Pirazzoli 1986). However, a connection between these notches and mean sea-level (msl) was

proven for some survey sites (Kline et al. 2014). Abrasion notches can potentially form near the breaking depth of waves and up to the storm-swash wave height, which is the maximum elevation that is reached by waves during extreme storm events (Pirazzoli 1986; Rovere et al. 2016). For simplicity we refer to notches without traces of bioerosion as abrasion notches in this study.

### 1.2 Bioeroding Organisms

Because bioerosion happens through chemical dissolution, most bioerosion notches form in carbonate rocks (Kershaw & Guo 2001; Rovere et al. 2016; Schneiderwind et al. 2016). The main bioeroding genera are bivalves, such as *Lithophaga*, limpets, chitons, sponges (*Cliona*) and sea urchins (Kázmér et al. 2015; Laborel & Laborel-Deguen 1994). They occur alongside bioconstructing organisms like barnacles, oysters and tube-building worms, which have a protective effect on the rock surface (Kázmér et al. 2015; Antonioli et al. 2015). All of these organisms may function as biological indicators of paleo sea-level, since they have adapted to specific conditions of temperature, light intensity and water coverage (Laborel & Laborel-Deguen 1994). Due to their adaptation, individuals of a species are generally found in distinct, sub-horizontal belts in a certain elevation relative to msl (Laborel & Laborel-Deguen 1994, Rovere et al. 2015, Schneiderwind et al. 2016).

The limestone boring lamellibranches *Lithophaga* create dumbbell-shaped cavities within limestone surfaces to escape predators. An individual *Lithophaga* widens the cavity it has settled in according to its growth but cannot expand the opening and is therefore unable to abandon its boring. *Lithophaga* need to be permanently submerged. The upper limit of their living range is located between msl and mean low water (mlw), while their lower limit reaches depths of up to 30 m (Pérès 1982). However, the highest concentration of *Lithophaga* borings are usually found within the top few meters below sea-level (Rovere et al. 2015). While the shell and soft tissue of the organism are rarely preserved, their borings have a good preservation potential. The ichnotaxon that is used to describe dumbbell-shaped borings like the ones produced by *Lithophaga* is called *Gastrochaenolites* (Bromley and Asgaard 1993).

Sponges are sessile filter feeders (Miller 2007). Boring sponges create millimeter wide openings in a limestone surface, which are interconnected by a network of small tubes and chambers below the surface. The whole structure only penetrates a couple of millimeters deep and is therefore prone to erosion. The openings, called papillae, function as water drainage system for the sponge (Nava and Carballo 2008, Westerheide and Rieger 2007). Most rock-boring sponges belong to the taxon *Demospongia* (Westerheide and Rieger 2007). In ichnology the traces of boring sponges are summarized into the ichnotaxon *Entobia* (Bromley and Asgaard 1993). Boring sponges are usually restricted to the subtidal and have only rarely been documented within the intertidal zone (Abad et al. 2013).

Oysters are bioconstructing, sessile bivalves that attach themselves to hardgrounds (Kázmér et al. 2015). Because of their tolerance to most ecological stressors like varying salinity or dryfalling, oysters have a very wide living

range (Laborel and Laborel-Deguen 1994). However, their living range can be regionally limited by the occurrence of natural enemies or species-specific behavior (Rovere et al. 2015). A comparison between fossil oysters and the living colonies at the same coastline can help tie them to a certain elevation relative to sea-level (Rovere et al. 2015). A <sup>14</sup>C-dating approach on the oysters at outcrop A failed due to recrystallisation of the sample.

Tube building worms *Pomatoleios kraussii* are sessile organisms that surround themselves with calcareous tubes attached to a hardground (Belal and Ghobashy 2012, Westerheide and Rieger 2007). Their preferred areas of settlement are in a sheltered position with weak currents and a low sediment income (Straughan 1969). The living range of these worms reaches from the subtidal to the intertidal zone (Belal and Ghobashy 2012, Shalla and Holt 1999).

Among barnacles only the families *Balanidae* and *Chthamalidae* are useful as sea-level indicators, since most other families have very wide living ranges (Rovere et al. 2015). *Balanidae* settle near msl between the middle and lower intertidal zones (Laborel and Laborel-Deguen 1994, Rovere et al. 2015). While their preservation potential is low on a submerged surface, it increases once they are emerged above sea-level.

## 2 Regional setting

The Sultanate of Oman is located on the Arabian Peninsula and shares borders with Yemen, Saudi Arabia and the United Arab Emirates (Figure 1). Its coastline adjoins to the Gulf of Oman in the northeast and the Arabian Sea, as part of the Indian Ocean, in the southeast and east. Much like the rest of the Arabian Peninsula Oman's climate is

hyper-arid with annual precipitation below 50 mm in all areas apart from the mountain ranges, where annual precipitation peaks at 250 mm (Al-Charaabi & Al-Yahyai 2013; Kwarteng et al. 2009).

Our study area is Sur Lagoon at the northeastern coastline of Oman (Figure 1). This coastline is divided by a prominent tectonic feature: the Qalhat Fault, which is an active, normal fault, meeting the coastline at a shallow angle close to the ancient city of Qalhat. Qalhat lies on the coast 22 km northwest of Sur Lagoon (Figure 1). The crustal block north of the Qalhat Fault shows signs of neotectonic activity and uplift, described in detail by Ermertz et al. (2019). The crustal block south of the Qalhat Fault, where Sur is located, is tectonically stable (Kusky et al. 2005).

Sur is a harbour city located on a Holocene barrier spit. The horseshoe-shaped Sur Lagoon covers roughly 12 km<sup>2</sup>, has a narrow outlet to the sea and two peninsulas reaching into it from the west (see Figure 1). The majority of the rocks outcropping around Sur Lagoon are Miocene limestone or marl called the Sur Formation (Fournier et al. 2006). These beige to light-yellow coloured carbonate rocks are dipping sea-wards with a 3° angle and are locally fossiliferous. Predominately on the western side of Sur Lagoon a second bedrock-lithology occurs: Quaternary alluvial deposits, interpreted as fanglomerates. These deposits are polymictic conglomerates with granule to cobble sized, well rounded clasts. The clasts are limestone, sandstone, quartzite and subordinate chert within a medium- to coarse-sand matrix.

The maximum tidal range at the northeastern coast of Oman is about 3 m (McLachlan et al. 1998). The area is therefore classified as mesotidal. The tides in Oman are

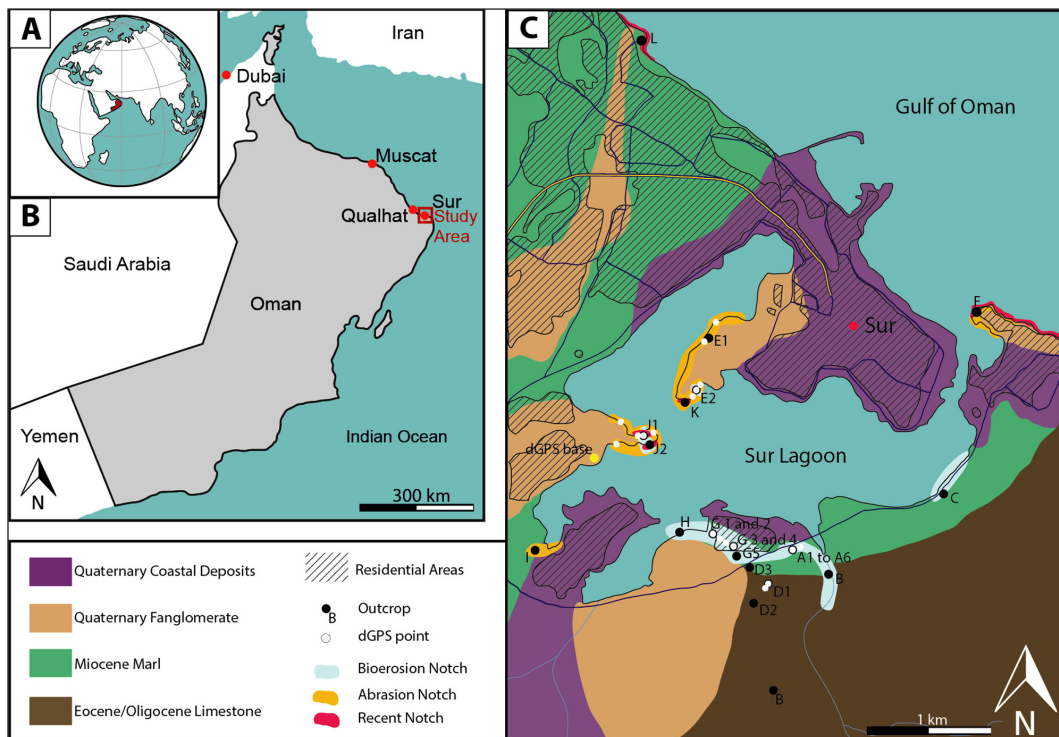


**Figure 1:** **A)** Location of the Sultanate Oman on a world map (marked in red). **B)** More detailed map of the Sultanate Oman. The Study Area is located in the city of Sur at the northeastern coastline and the ancient city of Qalhat 22 km northwest of Sur. **C)** The city of Sur and its hippocrepiform lagoon with occurrences of coastal notches, differential GPS measurements and profile-locations.

semi-diurnal, with two highs and lows per day. The tidal range inside Sur Lagoon is significantly smaller than in the open sea with an average tidal range of 1.2 m, which classifies as a microtidal environment. During low tide the lagoon is mostly water-free so that fine-grained sandy and silty deposits are exposed (Donato et al. 2009). Coastal notches are observed above high tide in the South, South-West, and West of the lagoon. At outcrops A, G, E and J the paleo notches are in some ways associated with beachrocks. These are cemented, sandy or gravelly beach deposits, described in detail by Falkenroth et al. (2019b).

### 3 Methods

At twelve locations around Sur Lagoon coastal notches and/or bioerosion-horizons occur. Outcrops are numbered with the letters A to L. This study focusses on eight outcrops, which we deem to be most useful for sea-level reconstruction, these are outcrops A, D, E, F, G, J, K and L, as those show the most complete preservation of notch shape or biological markers. At each of the outcrops the notch shape, biological markers and spatial relationship to other rock facies are unique. On the paleo notches we mapped the morphology of the notches and measured the distance between the notch roof and the notch floor, which is referred to as notch width in this study. Whenever there is bioerosion present, be it within, above or below the notch shape we measured the range of occurrence for each organism group. When possible, we linked the documented traces to a certain tracemaker, when the trace can stem from a whole taxon we use the assigned ichnotaxa to classify the traces. The information on notch habitus and organism zonation is presented as profiles. Depending on the lateral extend of an outcrop the number of measured profiles per outcrop varies, as indicated by the numbers

accompanying the outcrop letter (i.e. A1, A2, etc.). Overall 24 profiles were measured.

To measure the notch width and vertical extend of an outcrop we used a Handheld Laser Distance Meter (HLD) (see Kázmér & Taboroši 2012a). The model Leica Disto D8 was used to obtain the height and horizontal length of the notch. The uncertainty of the measurement device is around  $\pm 1$  mm with a measurable maximal distance of 200 m.

To achieve absolute elevations, we used a Differential GPS (DGPS) and measured the highest *Lithophaga* boreholes at each profile location. This measurement was then used as a reference point to calculate the absolute height of all features of the profile, namingly organism zonation and notch morphology. The dGPS (Leica GS15) was used in a real-time kinematic mode. The dGPS contains of two paired antennas and reaches an accuracy of 0.02 m or less in x-, y-, and z-direction relative to the base station. Coordinates are presented as meters within the Universal Transverse Mercator (UTM) projection, Zone 40Q using the WGS 1984 reference ellipsoid. To calculate the absolute height, the sea-level was first measured at different tidal datums and normed to msl. Afterwards the difference in height between msl and the *Lithophaga* boreholes were examined.

The distribution and position of trace fossils within the bioerosion notch was surveyed using measuring tape. The lowest and highest points of bioerosional features on the rock surface, as well as the distribution of every organism were measured relatively to the highest *Lithophaga* boring for which an absolute height is available. Furthermore, the positions of the notch apex, notch roof and the notch floor relative to the highest *Lithophaga* boring were measured (Figure 2a).

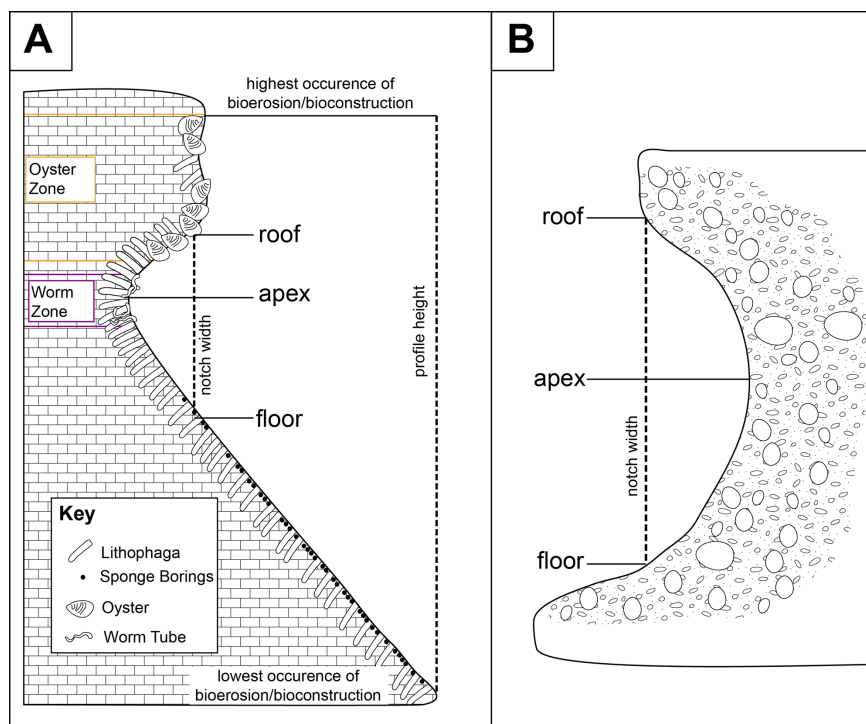


**Figure 2:** A) Example for the measurements on the bioerosion notch. B) Measurements performed on the abrasion notch.

The tape-measurements lies within a confidence interval of  $\pm 4$  cm.

In **Table 1** each height is presented with an error, which is composed of the errors associated with each individual measurement that was conducted to calculate the height value.

To reconstruct short-term sea-level fluctuations the range of biological indicators within paleo notches is interpreted relative to the shape of the notch and other geomorphological sea-level markers, like beachrock. The morphology and faunal association of the recent notches constitute a meaningful comparison when interpreting paleo notches, which is why the recent notches were also investigated as part of this study (see **Table 3**). Recent notches are those notches, which are located in the intertidal zone nowadays and are inhabited by recent organisms.

### 3.1 <sup>10</sup>Be Dating of the Fanglomerates in Sur

For the age constrain on the formation of the paleo notches we dated the alluvial conglomerates that form the peninsulas in Sur Lagoon (see **Figure 1**). See section 4 for details on the spatial relationship of these conglomerates with each of the coastal notches. We collected five quartzite cobbles from the fan surface, which were then dated using cosmogenic radionuclide <sup>10</sup>Be. To avoid material that experienced postdepositional re-location or overturning, sampling was carried out in a distance to channels or gullies. We chose cobbles that were partly buried in a sandy matrix and show a smooth, flat surface, without ventifacts implying that these cobbles most likely remained in situ since initial deposition. Topographic shielding factors for each sample site were measured in the field. Since most quartzite cobbles have smoothed flat surfaces, we assumed a zero erosion rate. The <sup>10</sup>Be concentrations in 5 cobbles were analysed. The samples were prepared as Accelerator Mass Spectrometry (AMS) targets at the Institute of Geology and Paleontology, University of Münster, Germany, following the standard procedures outlined in Schmidt et al. (2011). A blank as well as one DWA 98002 quartz standard material sample was prepared to ensure quality control (Falkenroth et al. 2019a). All targets were measured at Cologne AMS (Dewald et al. 2013) and normalised to the <sup>10</sup>Be standards of Nishiizumi et al. (2007). The <sup>10</sup>Be concentrations were determined following the subtraction of reagent blanks, which were prepared along with the samples. <sup>10</sup>Be exposure ages are derived from 'The online exposure age calculator formerly known as the CRONUS – Earth online exposure age calculator'; version 3.0.2 (Balco et al. 2008), using the St-scaling (Stone 2000) and the time-dependent LSDn scaling factor (Lifton et al. 2014). All input parameters are listed in the supplementary dataset (Falkenroth et al. 2019a).

For our age model of the formation of paleo notches we used the data of our own dating survey in combination with data from the literature. Mauz et al. (2015) have dated beachrock in Sur Lagoon via optical stimulated luminescence to an age of  $80 \pm 3$  kyr.

## 4 Results

### 4.1 General Observations

Three kinds of sea-level indicators, which are coastal notches, traces of bioerosion and beachrocks, are found at

twelve outcrops in the study area. It can be noted that the upper limit of bioerosional traces (with or without notch shape) lies roughly at 4.31 m amsl at all outcrops (see **Figure 3**). All notches, that show a notch shape, but no sign of bioerosion have an upper limit between 2 and 3 m amsl (see **Figure 4**). And all notches that are still inhabited by organisms today and whose formation is thereby ongoing have an upper limit between msl and 1 m, as expected (see **Figure 5**). Those three categories, with special emphasis on the bioerosion traces, are described below. Together with each category we also describe the substrates and the spatial relationship to other sea level indicators such as beachrocks. Beachrocks occur at three outcrops in Sur Lagoon (A, J and E1).

### 4.2 Recent notches

We observe four different coastal notches that are located within the current intertidal zone and thereby still inhabited by a faunal community. The notch-forming processes are still ongoing in these cases. The active notches occur at outcrops J, F, K and L. While L and F are located outside of Sur Lagoon (L) or at the very edge of the entry (F), K is located on the northern and J on the southern peninsula (see **Figure 1**). The notches within Sur Lagoon (outcrops J and K) are significantly less well developed than the observed paleo notches, they are less wide and deep and show a smaller biodiversity. On the other hand the notches that are located in more exposed settings outside the Lagoon (F and L) show a closer resemblance to the investigated paleo-notches with a more similar shape and width.

The recent notches at outcrops J and K have developed within the same limestones as most of the paleo notches that show bioerosional features. The recent notch at outcrop F formed within the fanglomerate, the one at outcrop L within a raised coral reef platform. For details of the notch characteristics and organism distribution see **Figure 5** and **Tables 1** and **3**.

Because the position of oyster colonization relative to msl is often depending on the species and regional habitat characteristics we investigated the living oyster colonies around Sur Lagoon. Because of their sensitivity to environmental factors and the plasticity of the shell, oysters are generally difficult to identify based on their shell morphology (Chesalin et al. 2012). Previous studies of oyster populations along the coastline of Oman with DNA-sequencing show that the most common species is *Saccostrea cucullata* (Chesalin et al. 2012). We noted that recent oyster colonies form a very densely populated, 0.2 to 0.3 m wide congregation at high tide level in addition to the spotted, wider distribution of single individuals. The oyster specimen show a flat, almost round upper valve and a larger lower valve as typical of *Saccostrea cucullata*.

### 4.3 Abrasion Notches

Notches without indication of bioerosional activity occur on outcrops E, F and J. Their appearance is almost exclusive to the north-western margin of Sur Lagoon. The bedrock in which the abrasion notches formed are either fanglomerate (F, E2) or beachrock (E1, J), both of which are described more detailed in sections 4.3.1 and 4.3.2.

**Table 1:** Overview over the observed coastal notches with geographic locations, description and elevation relative to msl.

Outcrop Profile No.	GPS (UTM WGS84 Zone 40Q)	Short Description	Notch Apex Elevation [m amsl]	Notch Roof Elevation [m amsl]	Notch Floor Elevation [m amsl]	Notch width or extend of the bioerosional horizon [m]
A	A1 759913 2495752	Tidal Notch with trace fossils in limestone substrate, u-shaped notch	4.13 ± 0.1	4.23 ± 0.06	4.03 ± 0.06	0.20 ± 0.01
	A2 759912 2495754		3.95 ± 0.1	4.27 ± 0.06	3.64 ± 0.06	0.63 ± 0.01
	A3 759916 2495762		3.84 ± 0.1	4.26 ± 0.06	3.43 ± 0.06	0.83 ± 0.01
	A4 759922 2495768		3.89 ± 0.1	4.34 ± 0.06	3.44 ± 0.06	0.9 ± 0.01
	A5 759928 2495771		3.88 ± 0.1	4.25 ± 0.06	3.51 ± 0.06	0.81 ± 0.01
	A6 759936 2495777		3.91 ± 0.1	4.29 ± 0.06	3.54 ± 0.06	0.75 ± 0.01
B	B 760059 2495519	Limestone surface with trace fossils, no notch shape		No dGPS measurement	No dGPS measurement	0.45 ± 0.06
C	C 760990 2496380	Notch with trace fossils in limestone, u-shaped notch		No dGPS measurement	No dGPS measurement	0.72 ± 0.01
D	D1 759656 2495583	Limestone surface with trace fossils, no notch shape	No apex	4.42 ± 0.06	3.47 ± 0.06	0.95 ± 0.1
	D2 759591 2495455	Bioerosional horizon in limestone, only notch roof		No dGPS measurement	No dGPS measurement	0.53 ± 0.01
	D3 759553 2495652	Bioerosional horizon covered by a buildup of tube-building worm remains	No apex	4.28 ± 0.06	4.02 ± 0.06	0.26 ± 0.1
E	E1 758822 2497588	Notch without trace fossils in sandy beachrock	1.75 ± 0.1	2.96 ± 0.06	1.1 ± 0.06	1.86 ± 0.01
	E2 758752 2497122	Notch without trace fossils (AN), a bioerosional horizon (BH) is visible above the notch, substrate of both is fanglomerate	BH: no apex AN: 1.5 ± 0.1	BH: 4.39 ± 0.06 AN: 2.43 ± 0.06	BH: 4.15 ± 0.06 AN: 0.57 ± 0.06	BH: 0.24 ± 0.01 AN: 1.86 ± 0.01
F	F1 761145 2498062	Notch without trace fossils in fanglomerate substrate	2.50 ± 0.1	2.74 ± 0.06	1.03 ± 0.06	1.71 ± 0.01
	F2 761145 2498076	Actively forming u-shaped tidal notch in fanglomerate	0.16 ± 0.1	0.54 ± 0.06	-1.1 m ± 0.06	1.64 ± 0.01
G	G1 7590577 2495810.8	Notch with trace fossils in limestone substrate	3.8 ± 0.1	4.1 ± 0.06	3.34 ± 0.06	0.76 ± 0.01
	G2 759061.2 2495807.8		3.75 ± 0.1	4.2 ± 0.06	3.35 ± 0.06	0.85 ± 0.01
	G3 759180.5 2495737.7		3.92 ± 0.1	4.34 ± 0.06	3.5 ± 0.06	0.84 ± 0.01
	G4 759286.6 2495717.7		4.14 ± 0.1	4.44 ± 0.06	3.84 ± 0.06	0.6 ± 0.01
	G5 759275.9 2495652.3		4.03 ± 0.1	4.33 ± 0.06	3.83 ± 0.06	0.5 ± 0.01
H	H 758755.2 2495780.4	Bioerosional horizon in limestone, no notch shape		No dGPS measurement	No dGPS measurement	0.6 ± 0.06
I	I 757440.7 2495440.8	Bioerosional horizon without notch shape		No dGPS measurement	No dGPS measurement	0.45 ± 0.06

(Contd.)

Outcrop Profile No.	GPS (UTM WGS84 Zone 40Q)	Short Description	Notch Apex Elevation [m amsl]	Notch Roof Elevation [m amsl]	Notch Floor Elevation [m amsl]	Notch width or extend of the bioerosional horizon [m]	
J	J1	758373.9 2496601.7	A bioerosional horizon without notch shape within a fanglomerate (BH), the fanglomerate is covered by sandy beachrock which shows an irregular shaped notch without trace fossils (AN), below the fanglomerate and the beachrock an active tidal notch forms within limestone (RN)	BH: no apex AN: 2.13 ± 0.1 RN: 0.83 ± 0.06	BH: 4.53 ± 0.06 AN: 2.76 ± 0.06 RN: 0.93 ± 0.06	BH: 3.87 ± 0.06 AN: 1.42 ± 0.06 RN: 0.73 ± 0.06	BH: 0.66 ± 0.1 AN: 1.34 ± 0.01 RN: 0.2 ± 0.1
J	J2	758385.7 2496554.5	A bioerosional horizon within the fanglomerate (BH) is visible above a v-shaped notch without trace fossils within the same substrate (AN), below the fanglomerate an active tidal notch forms within limestone (RN)	BH: no apex AN: 2.50 ± 0.1 RN: 0.73 ± 0.06	BH: 4.43 ± 0.06 AN: 3.13 ± 0.06 RN: 0.83 ± 0.06	BH: 4.03 ± 0.06 AN: 1.78 ± 0.06 RN: 0.63 ± 0.06	BH: 0.4 ± 0.1 AN: 1.35 ± 0.01 RN: 0.2 ± 0.01
K	K	758671.1 2496987.1	Actively forming, v-shaped tidal notch in limestone substrate	0 ± 0.1	0.29 ± 0.06	-0.44 ± 0.06	0.73 ± 0.01
L	L	757889.6 2500112.3	Actively forming, u-shaped tidal notch in a dead coral reef platform	0.47 ± 0.1	0.9 ± 0.06	-0.1 ± 0.06	1 ± 0.01
Averages Paleo Bioerosion Notches with standard deviation			3.93 ± 0.12	4.31 ± 0.1	3.69 ± 0.27	0.62 ± 0.22	
Averages Paleo Abrasion Notches with standard deviation			2.08 ± 0.4	2.80 ± 0.24	1.18 ± 0.4	1.62 ± 0.23	

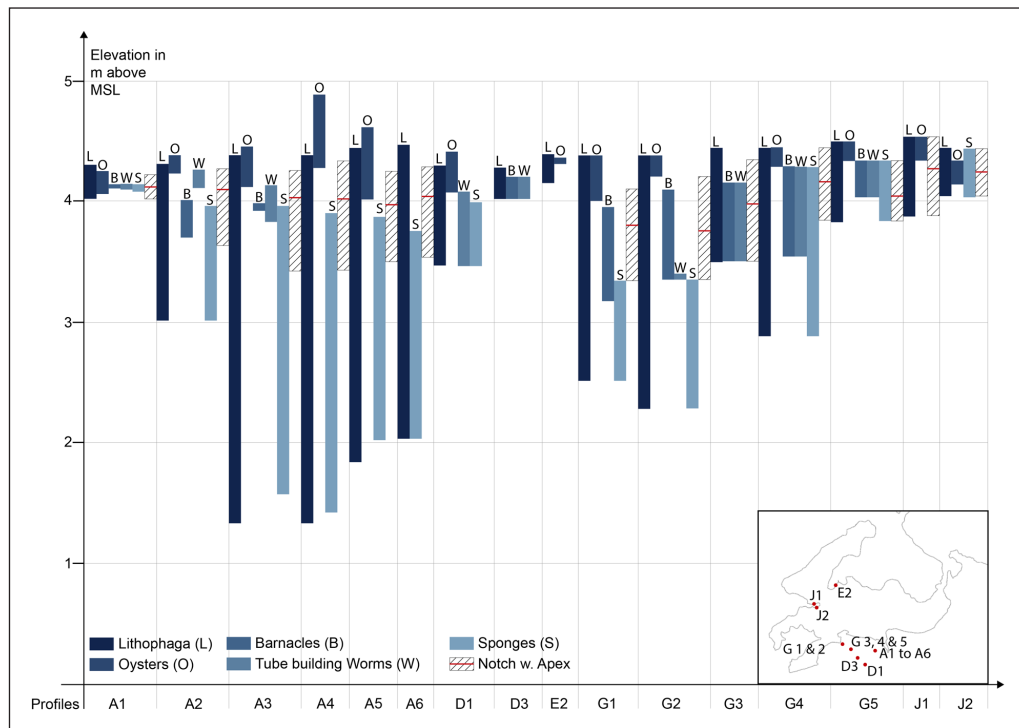


**Figure 3:** Trace fossil distribution, notch width and position relative to msl of the bioerosion notches near Sur. At locations D1, D3 and E2 no notch shape is observed but a bioerosion-horizon.

The characteristics of these abrasional notches are similar at all outcrops, displaying a round u-shape and a smooth surface. On outcrops E2, J1 and J2 bioerosional horizons are observed above the abrasional notches (see **Figure 6**). The floors of the abrasional notches are located between 0.57 m and 1.78 m above msl (amsl), the roofs are located between 2.43 m and 3.13 m on all documented outcrops. The average width of the abrasion notches is  $1.62 \pm 0.23$  m. A trend is notable: the best developed and widest abrasional notches are located on the northern peninsula (outcrop E), facing the centre of the lagoon, the smallest abrasional notches occur closer to the mainland at outcrop J. For details of the notch-characteristics see **Figure 4** and **Table 1**.

**4.3.1 Fanglomerates**

This conglomerate forms both of the peninsulas reaching into Sur Lagoon and also cover parts of the coastline (see **Figure 1**). They are interpreted as cemented, fluvial deposits since they lack any marine fossils and the limestone clasts, embedded in them, show no signs of bioerosion. The clasts are dominantly pebble-sized with lesser amounts of granules and cobbles. They primarily consist of limestone, but sandstone, quartzite and, least commonly, chert also occur. The matrix of this polymictic conglomerate is made of middle to coarse grained sand. Quartzite cobbles from this fanglomerate were dated using cosmogenic radionuclide  $^{10}\text{Be}$  (see **Table 4**). The dating results are scattered between  $153 \pm 43$  ka and  $371 \pm 38$  ka.

**4.3.2 Beachrocks associated with the abrasion notches**

At outcrops E1, J1 and J2 the abrasion notches formed within beachrocks (see **Figures 4** and **6**).

The beachrock at outcrop E1 comprises two lithofacies: one sandstone (thickness 2.15 m) and one conglomerate

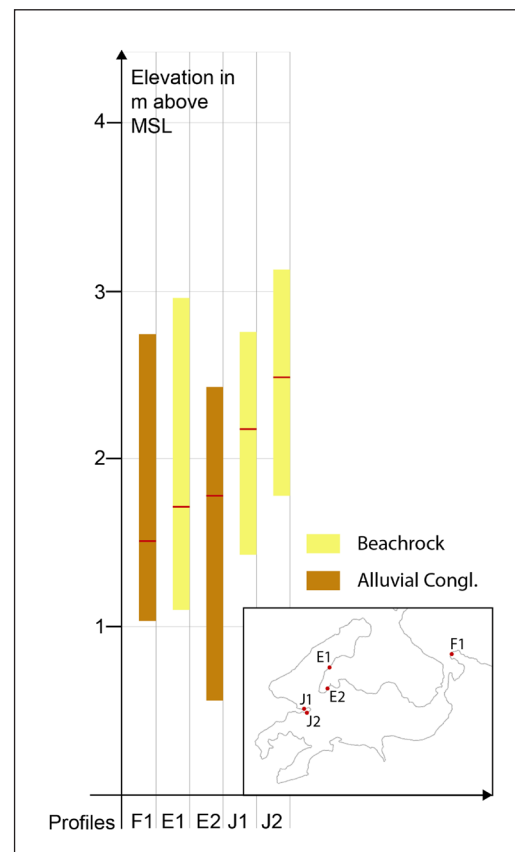


**Figure 4:** Location, substrate, width and elevation relative to msl of the abrasion notches around Sur Lagoon. The red stripe marks the position of the notch apex.

(thickness 0.17 m). The sandstone is massive, thickly bedded and consists of coarse to very coarse sand, consolidated by a sparitic, carbonate cement. The sediment is fossiliferous with remains of bivalves (including oysters),

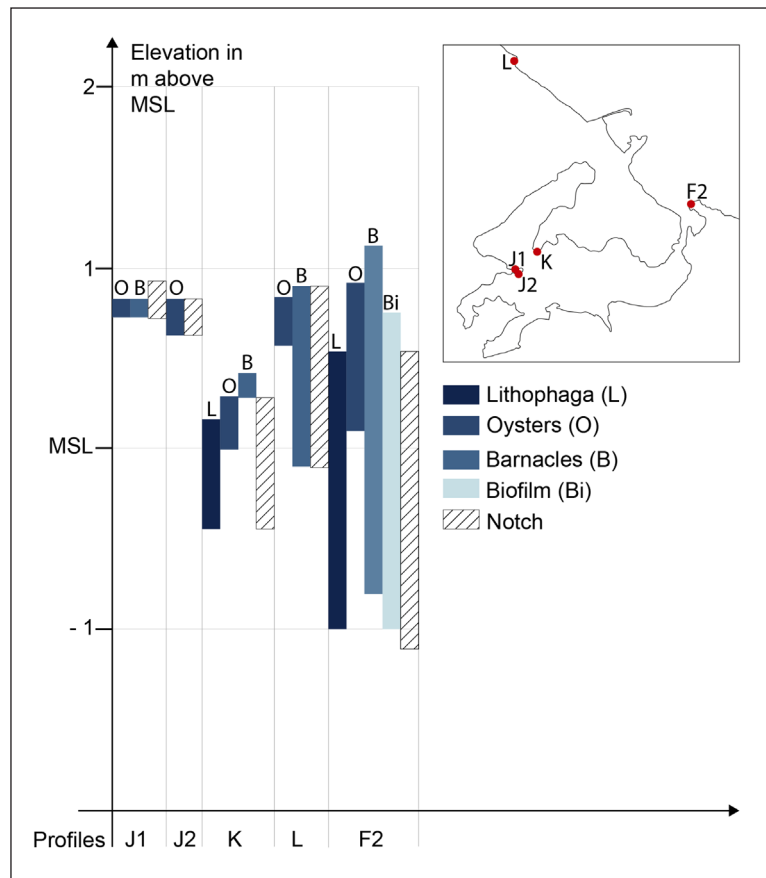


**Figure 5:** Faunal distribution, position, notch width (distance of roof and floor) and elevation relative to msl of recent bioerosion notches near Sur.

gastropods and corals. Most of these fossils are fragmented. Besides the fossils the sediment further contains granule- to cobble-sized limestone clasts. While cobble sized clasts occur concentrated in lenses or bands, pebbles and granules are spread out evenly throughout the layers. The clasts are angular to subangular and show signs of bioerosion, some are overgrown by barnacles or tube-building worms. The sediment is characterised by small-scale through cross-stratification. The sandstone-facies is overlain by a poorly sorted, matrix-supported conglomerate, which has a high fossil content and granule- to large pebble-sized limestone-clasts. Again, the clasts are subangular and show various signs of bioerosion like the sponge-trace *Entobia* or remains of tube-building worms. The notch formed entirely within the sandstone facies, with the notch floor laying at the same elevation as the base of the beachrock succession (1.1 m amsl).

The beachrock at outcrop J is a 2 m thick, intensely burrowed, moderately sorted, coarse sandstone. It comprises multiple conglomeratic lenses and bands as well as isolated clasts. The size of these clasts ranges from granules to small cobbles. Both, larger clasts and grains of the sandy matrix are angular. The sediment is fossiliferous, most common macrofossils are oyster-shells, but other gastropod-shells and bivalves do also occur. The observed burrows form a network and belong to the ichnogenus *Thalassionides paradoxicus*, which is usually created by arthropods.

Both beachrock deposits were cemented onto the surface of the fanglomerates that form the bedrock of the

peninsulas (see **Figure 6** and section 4.3.1). They were previously studied regarding their depositional environment and represent an upper shoreface facies (Falkenroth et al. 2019b).

#### 4.4 Bioerosion Notches

Occurrences of coastal notches formed by bioerosion are most common in the southern part of Sur Lagoon at outcrops A, C, G and H. The details of the notch characteristics at each outcrop as well as the distribution of the different groups of organisms are shown in **Figure 3** and **Table 2**. The notches are carved into the Miocene Sur Formation, which consists of limestones and marls with a varying clay-content (Wyns et al. 1992). The notch-shape is most prominently preserved at outcrops A and G. The bioerosion notches have a mean notch width of  $0.62 \pm 0.22$  m with an apex located averagely at  $3.93 \pm 0.12$  m above msl. Along the northern and western coastline of Sur Lagoon, namely at outcrops B, D, I, J and E, bioerosional horizons without a distinct notch-shape occur above the abrasional notch. The traces and remains of five groups of organisms are found associated with the bioeroded surfaces.

The five biological indicators that are of importance in this study are boring mussels of the genus *Lithophaga*, boring sponges of the genus *Cliona* and bioconstructors like oysters, the tube-building worm *Pomatoleius kraussii* and *Balanidae*, which are small crustaceans known as barnacles. The genera *Lithophaga* and *Cliona* are both bioeroding organisms and are responsible for the largest share of the observed traces. Oysters, the tube-building

**Table 2:** Organism distribution within the paleo bioerosion notches.

Outcrop Profile	<i>Lithophaga</i>			Oysters			Barnacles			Tube-building worms			Sponges		
	Lower limit [m amsl]	Upper limit [m amsl]	Lower limit [m amsl]	Upper limit [m amsl]	Lower limit [m amsl]	Upper limit [m amsl]	Lower limit [m amsl]	Upper limit [m amsl]	Lower limit [m amsl]	Upper limit [m amsl]	Lower limit [m amsl]	Upper limit [m amsl]	Lower limit [m amsl]	Upper limit [m amsl]	
A	A1	4.03 ± 0.06	4.32 ± 0.02	4.07 ± 0.06	4.26 ± 0.06	4.12 ± 0.06	4.15 ± 0.06	4.11 ± 0.06	4.16 ± 0.06	4.09 ± 0.06	4.15 ± 0.06	4.09 ± 0.06	4.15 ± 0.06		
	A2	3.02 ± 0.06	4.32 ± 0.02	4.24 ± 0.06	4.39 ± 0.06	3.71 ± 0.06	4.02 ± 0.06	4.12 ± 0.06	4.27 ± 0.06	3.02 ± 0.06	3.97 ± 0.06	3.02 ± 0.06	3.97 ± 0.06		
	A3	1.38 ± 0.06	4.32 ± 0.02	4.12 ± 0.06	4.46 ± 0.06	3.93 ± 0.06	3.99 ± 0.06	3.84 ± 0.06	4.14 ± 0.06	1.58 ± 0.06	3.97 ± 0.06	1.58 ± 0.06	3.97 ± 0.06		
	A4	1.34 ± 0.06	4.39 ± 0.02	4.29 ± 0.06	4.89 ± 0.06	None	None	None	None	1.43 ± 0.06	3.91 ± 0.06	1.43 ± 0.06	3.91 ± 0.06		
	A5	1.85 ± 0.06	4.45 ± 0.02	4.02 ± 0.06	4.62 ± 0.06	None	None	None	None	2.03 ± 0.06	3.89 ± 0.06	2.03 ± 0.06	3.89 ± 0.06		
	A6	2.04 ± 0.06	4.47 ± 0.02	None	None	None	None	None	None	2.04 ± 0.06	3.86 ± 0.06	2.04 ± 0.06	3.86 ± 0.06		
D	D1	3.47 ± 0.06	4.30 ± 0.02	4.08 ± 0.06	4.42 ± 0.06	4.02 ± 0.06	4.20 ± 0.06	3.47 ± 0.06	4.08 ± 0.06	3.47 ± 0.06	3.99 ± 0.06	3.47 ± 0.06	3.99 ± 0.06		
	D3	4.02 ± 0.06	4.28 ± 0.02	None	None	4.02 ± 0.06	4.20 ± 0.06	4.02 ± 0.06	4.20 ± 0.06	None	None	4.02 ± 0.06	None		
E	E2	4.15 ± 0.06	4.39 ± 0.02	4.31 ± 0.06	4.36 ± 0.06	None									
G	G1	2.51 ± 0.06	4.38 ± 0.02	4 ± 0.06	4.38 ± 0.06	3.17 ± 0.06	3.95 ± 0.06	3.35 ± 0.06	3.40 ± 0.06	2.51 ± 0.06	3.34 ± 0.06	2.51 ± 0.06	3.34 ± 0.06		
	G2	2.28 ± 0.06	4.38 ± 0.02	4.20 ± 0.06	4.38 ± 0.06	3.35 ± 0.06	4.09 ± 0.06	3.35 ± 0.06	3.40 ± 0.06	2.28 ± 0.06	3.35 ± 0.06	2.28 ± 0.06	3.35 ± 0.06		
	G3	3.5 ± 0.06	4.44 ± 0.02	None	None	3.5 ± 0.06	4.15 ± 0.06	3.5 ± 0.06	4.15 ± 0.06	None	None	3.5 ± 0.06	None		
	G4	2.88 ± 0.06	4.44 ± 0.02	4.28 ± 0.06	4.44 ± 0.06	3.54 ± 0.06	4.28 ± 0.06	3.54 ± 0.06	4.28 ± 0.06	2.88 ± 0.06	4.28 ± 0.06	2.88 ± 0.06	4.28 ± 0.06		
	G5	3.83 ± 0.06	4.49 ± 0.02	4.33 ± 0.06	4.49 ± 0.06	4.03 ± 0.06	4.33 ± 0.06	4.03 ± 0.06	4.33 ± 0.06	3.83 ± 0.06	4.33 ± 0.06	3.83 ± 0.06	4.33 ± 0.06		
J	J1	3.87 ± 0.06	4.53 ± 0.02	4.33 ± 0.06	4.53 ± 0.06	None									
	J2	4.03 ± 0.06	4.43 ± 0.02	4.13 ± 0.06	4.33 ± 0.06	None	None	None	None	4.03 ± 0.06	4.43 ± 0.06	4.03 ± 0.06	4.43 ± 0.06		

**Table 3:** Distribution of organisms within the actively forming notches near Sur Lagoon.

Outcrop Profile	<i>Lithophaga</i> (abandoned hole)			Oysters			Barnacles		
	Lower limit [m amsl]	Upper limit [m amsl]	Lower limit [m amsl]	Upper limit [m amsl]	Lower limit [m amsl]	Upper limit [m amsl]	Lower limit [m amsl]	Upper limit [m amsl]	
F	F2	-1 ± 0.04	0.54 ± 0.02	0.01 ± 0.06	0.92 ± 0.06	-0.8 ± 0.06	1.13 ± 0.06		
J	J1	None	None	0.73 ± 0.06	0.83 ± 0.06	0.73 ± 0.06	0.83 ± 0.06		
	J2	None	None	0.63 ± 0.06	0.83 ± 0.06	None	None		
K	K	-0.44 ± 0.04	0.16 ± 0.02	0 ± 0.06	0.29 ± 0.06	0.29 ± 0.06	0.42 ± 0.06		
L	L	None	None	0.75 ± 0.06	0.84 ± 0.06	-0.1 ± 0.06	0.9 ± 0.06		

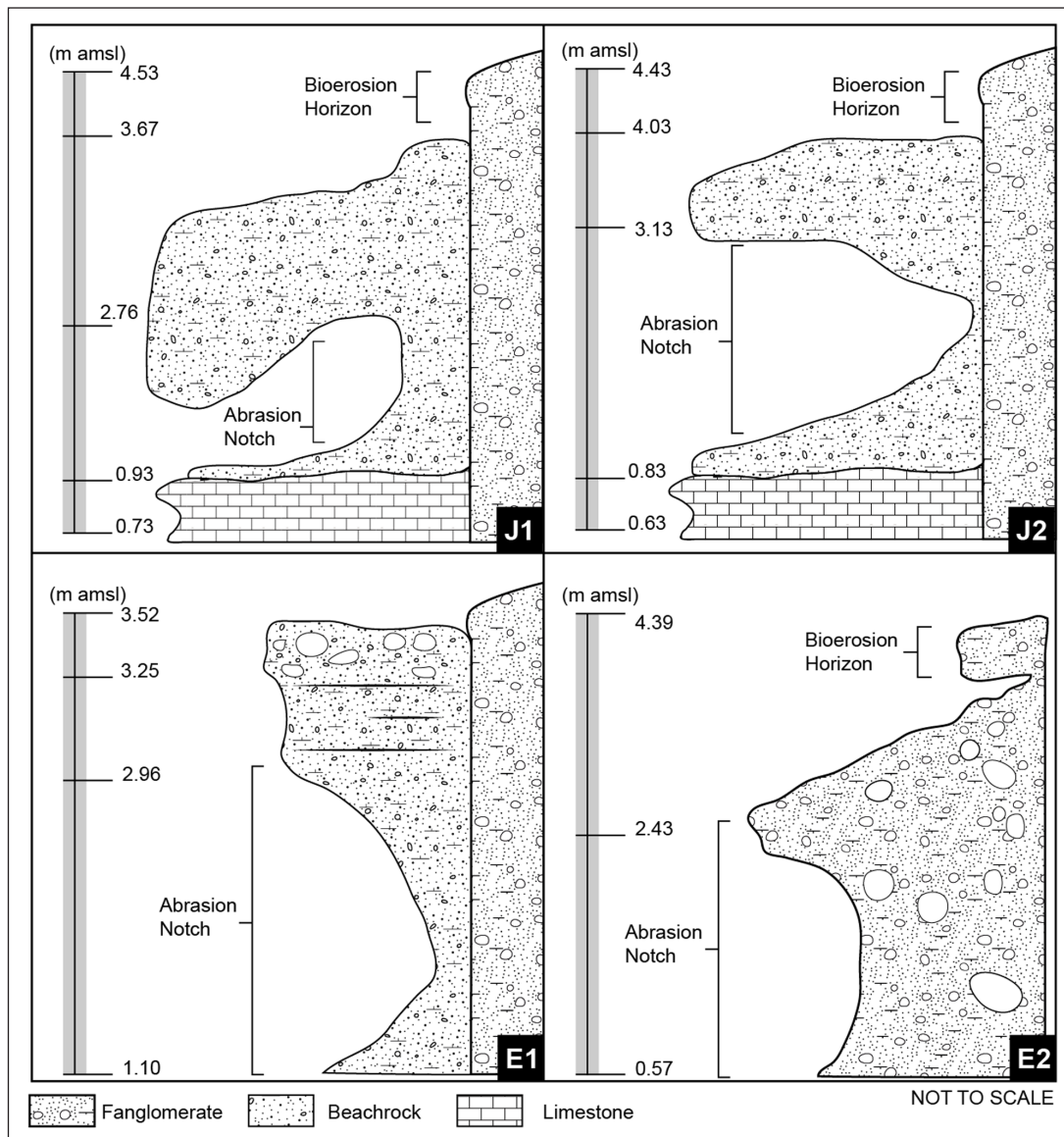


**Figure 6:** Spatial relationship of bioerosion horizons, abrasion notches and beachrocks at outcrops E1, E2, J1 and J2.

**Table 4:** Results from cosmogenic nuclide dating.

Sample Name	Sample Location	St-scaling		LsDn-scaling	
		Age (ka)	External Error (ka, 1σ)	Age (ka)	External error (ka, 1σ)
TD13-009a	22,5821 59,4518	201	22	209	20
TD13-009b	22,5821 59,4518	371	38	391	33
TD13-009c	22,5821 59,4518	342	31	358	26
TD13-009d	22,5821 59,4518	182	18	191	16
TD13-009f	22,5821 59,4518	153	43	164	45
Average		250	99	263	104

worms and barnacles are bioconstructors and common inside and above the bioerosion notch.

#### 4.4.1 Biological Indicators

In the study area, *Lithophaga* boreholes are present below, inside and above the notch and therefore display the greatest vertical propagation. They are occurring in large

quantities and are the main driver of erosion within the bioerosion notch (Figure 7a). The diameter of the boreholes varies from 0.5 cm to 2.5 cm and indicates different generations of *Lithophaga*. The depth of the traces is not consistent and ranges from millimetres to centimetres. Sponge borings occur in many of the measured profiles (Figure 7b). They mostly appear beneath the notch floor

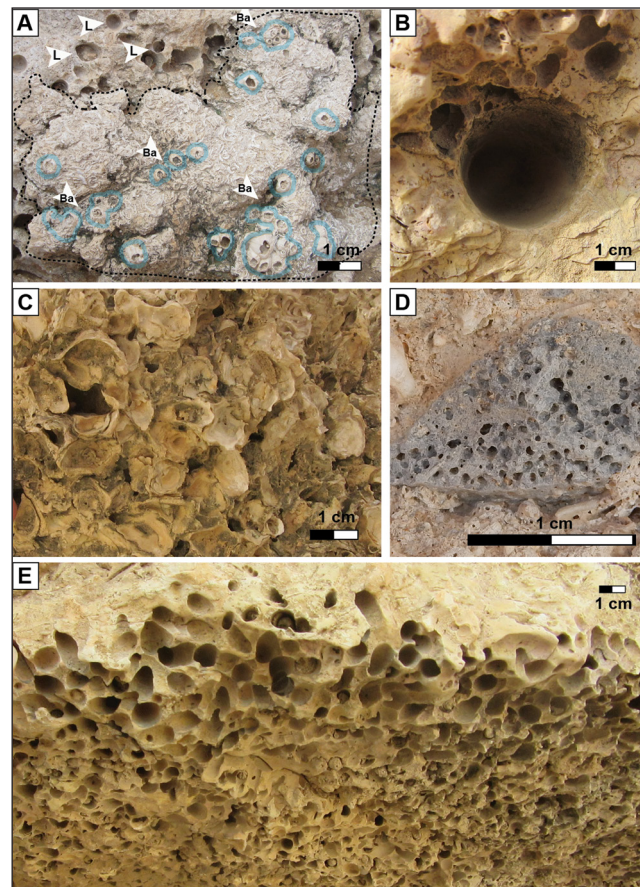


**Figure 7:** Fossil traces and remnants found inside the bioerosion notch. **A)** *Lithophaga*-bored surface overlain by barnacle-worm crust. [L]: *Lithophaga* [Ba]: Barnacles [dashed line]: worm crust, worm tubes probably by *Pomatoleios kraussii*. **B)** Large *Lithophaga* borehole exhumed by break off of the rock, surrounded by smaller holes of a later generation and the tracefossil *Entobia* (sponge boring). **C)** Oyster crust on notch roof at outcrop G. **D)** Sponge borings on a limestone pebble, ichnogenus *Entobia*. **E)** *Lithophaga*-drilled notch visor at outcrop G.

but often reach up to the middle of the notch near the apex (**Figure 3**). The depth of their boreholes is rather small and in the range of several millimetres. The boring pattern is an interconnected network of small chambers below the rock surface. On the surface the borings appear like a number of millimetre scale holes, which are close to one another but not connected. In ichnology, traces of boring sponges belong to the ichnogenus *Entobia*. The calcareous tubes of the bioconstructive *Pomatoleios kraussii* worm are either present inside of *Lithophaga* boreholes or located on the rock surface. In some locations thick ledges of worm tubes and barnacles cover up *Lithophaga* boreholes. The tubes are about 2 cm long and 2 mm in diameter. In this study remnants of barnacles of the family *Balanidae* commonly occur in the same areas as *Pomatoleios kraussii*. The shells are a few millimetres to 1 cm in diameter and their cover plates are missing. In some of the measured profiles barnacles occur, like *Pomatoleios kraussii*, inside of *Lithophaga* boreholes. Oyster shells are the most common bioconstructor and are present in many of the surveyed profiles. Because of their morphological variability oysters are difficult to identify to species level. The oysters are rather small with a diameter of 3 cm to 4 cm. They have roundish shells with smooth and flat upper valves. The fossil oysters resemble the genus *Sacostrea cucullata*, which is most common along the coastline

of Sur nowadays. They are always situated in the upper parts of the profile, normally near the roof of the notch or above. Only at outcrops C and H they are forming a band near the apex of the notch. Nevertheless, they appear generally between the middle of the notch and several centimetres above the roof. The preservation of the oyster shells is very variable, depending on their location and protection against weathering and mechanical erosion.

#### 4.4.2 Beachrocks associated with the Bioerosion Notches

At outcrop A the bioerosion notch crops out next to a 1.8 m thick beachrock-succession (see **Figure 8**). Additionally, there is a 0.2 m thick layer of similar beachrock cemented onto the surface inside the notch, which is similar to the sandstone facies of the larger beachrock outcrop and possibly, but not unequivocally, of the same age and origin (see **Figure 8**). It never exceeds a thickness of 0.2 m, which makes an allocation to a certain depositional environment difficult. In the larger outcrop a sandy beachrock discordantly overlays the fanglomerates (see **Figure 8**). The contact represents a depositional hiatus as shown by bioerosional traces of the *Trypanites*-ichnofacies, which have penetrated the surface of the conglomerate.

The sandstone is over 1 m thick, layered and consists of alternating bands of very coarse, coarse and medium sand. Lenses of larger clasts (granules to pebble size)

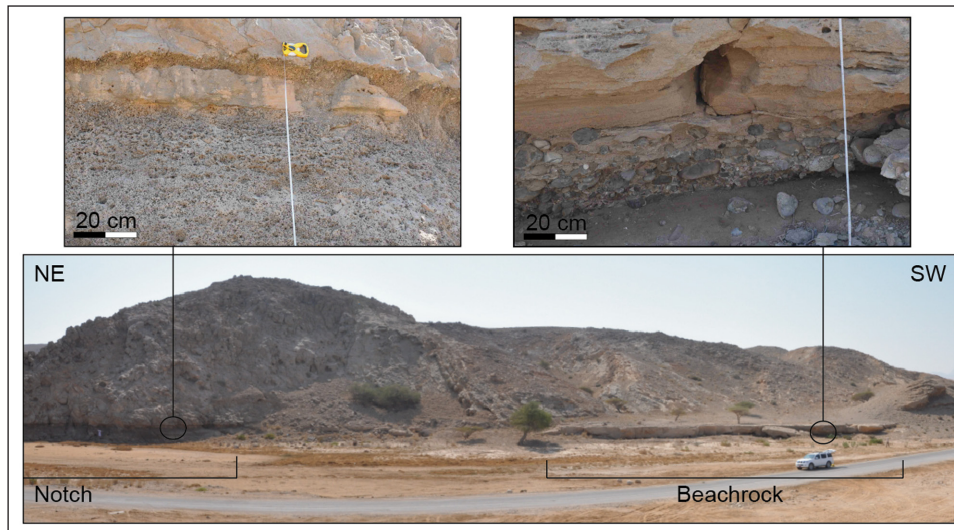


**Figure 8:** Overview over outcrop A with the bioerosion notch in the northeast and the beachrock in the southwest. Detailed photographs of the 20 cm thick beachrock within the notch (upper left) and the contact between the fanglomerates and the sandy beachrock (upper right).

occur as well as single floating limestone clasts and fossils. The clasts are angular to subrounded. Dislocated oyster shells, other bivalves and gastropods were identified. Furthermore, the coarse grained bands show a high amount of shell debris. Observed structures are parallel lamination, small scale tabular cross stratification and lenticular bedding. The sediment locally shows a high degree of bioturbation. At the north-eastern end of the outcrop the bed shows a section of symmetrical wave ripples with upbuilding of bidirectional cross lamination. At the bottom of the layer, a large tube-shaped burrow (6 cm wide and at least 80 cm long) was observed. The structure is cylindrical and shows a smooth wall with a 1 cm thick lining. This trace belongs to the ichnogenus *Palaeophycus heberti*, which can be produced by a number of animals such as *polychaetes*, *annelids* or *arthropods*, a larger size often pointing towards the latter. A facies analysis conducted by Falkenroth et al. (2019b) has allocated this beachrock to a lower foreshore facies overlain by an upper foreshore facies and thereby representing a regressional succession. The beachrock is located between 3.7 m and 2.4 m amsl.

This sandstone, was dated in a previous study by Mauz et al. (2015) to an age of  $80 \pm 3$  ka (sample ID: 565), using Optically Stimulated Luminescence (OSL).

## 5 Interpretation and Discussion

### 5.1 The age of the paleo notches in Sur Lagoon

Two dating results are available to produce an age constraint on the paleo notches in Sur Lagoon: the beachrock at outcrop A and the fanglomerate that forms a large share of the bedrock in Sur Lagoon. The fanglomerate gives a maximum age for the formation of the paleo notches as it becomes clear from their spatial relationship that its deposition must have preceded notch formation. For the abrasion notches this is obvious since at outcrops E2 and F1 they are carved into the fanglomerate, and at outcrops E1, J1 and J2 are carved into beachrocks that were cemented onto the surface of the fanglomerate (see

**Figure 6**) and therefore have to be younger. In case of the bioerosion traces the case is similar at outcrops E2, J1, and J2, where the traces occur directly on the surface of the fanglomerates and the traces penetrate both limestone clasts and the carbonatic cement that binds the fanglomerate together.

On outcrops where bioerosion traces occur but the fanglomerates do not (A, B, C, D, G, H and I) the age relationship is less obvious. However, it is the case that all traces of bioerosion show the same upper limit of  $4.31 \pm 0.1$  m amsl and thereby most likely represent the same paleo sea-level highstand.

The cosmogenic nuclide dating results for all samples are shown in **Table 4**. Since the LSDn-scaling results differ only by less than 10% and for reasons of simplicity, the reported ages in the text are based on St-scaling. The dating results of the fanglomerate samples are quite scattered, ranging from  $153 \pm 43$  ka to  $371 \pm 38$  ka. This can be due to either underestimation of the ages, caused by reworking or stronger erosion than expected, or overestimation of the ages, caused by inherited ages of the samples. For a conservative approach we will focus on the oldest date of  $371 \pm 38$  ka for the following argument.

The beachrock, which was dated to an age of  $80 \pm 3$  ka by Mauz et al. (2015) represents a minimum age for the formation of the paleo notches, as from their spatial relationship and the condition of the beachrock it is clear that it is younger or of the same age as the notch. The beachrock at outcrop A is located at a similar elevation as the bioerosion notch at outcrop A, with its upper limit positioned at 3.7 m amsl. If the beachrock was older than the notch, it would have been submerged during notch formation. Being immersed in sea water over an extended period of time would have altered the beachrock. The outcrop however shows no signs of reworking or erosion by waves, colonisation by marine organisms, such as the bioeroders and encrusters that heavily colonised the limestone surface next to it, or recrystallisation processes in its cements that can be linked to a water filled porespace. On

the contrary, the cements even show microstalgtites and meniscus cements that are indicative of constant wetting and drying but not permanent submergence (Falkenroth et al. 2019b).

While it cannot be stated without doubt that the sandy material within the bioerosion notch at outcrop A is the same deposit than the beachrock next to it, it has similar characteristics and shows that a sandy beachrock has formed here subsequent to notch formation.

All this makes a compelling case that the age obtained from this beachrock deposit is indeed a minimum age for formation of the bioerosion notch. This leaves us with a timeframe between  $371 \pm 38$  ka and  $80 \pm 3$  ka for the formation of the bioerosion notches in Sur Lagoon. It is known that the formation of a coastal notch requires an extended period of sea-level stillstand (Hearty et al. 2007). Three interglacial periods, the marine isotope stages MIS 9, MIS 7 and MIS 5 fall within the named timeframe.

During MIS 9 global sea-level peaked twice, one around 331 ka and once around 310 ka with global and rose to a level between  $-3$  m and  $+8$  m compared to today (Sidall et al. 2006). However, it is very unlikely that a sharp profile like a notch shape would survive denudation, dissolution and weathering over 330 ka (Hearty et al. 2007).

During MIS 7 there were three periods when eustatic sea-level approached the present level (Bintanja et al. 2005). Nevertheless, a comprehensive review of MIS 7 global sea-level data has shown that the sea-level highstands during MIS 7 peaked at  $-15$  m and  $-5$  m (Sidall et al. 2006), which is nowhere near the  $+3.93$  m we observe for the coastal notches in Sur Lagoon.

This leaves MIS 5 as only plausible interglacial for the formation of the paleo notches in Sur. MIS 5e is the only substage within MIS 5 that shows higher global sea-level than today ( $6 \pm 3$  m, Sisma-Ventura et al. 2017, Sidall et al. 2006).

### 5.2 Formation of the Abrasion Notches

The formation of abrasion notches is not bound to a tidal datum (Pirazzoli 1986), instead a correlation between wave height and notch width can be noted (Trenhaile, 2015). If an abrasion notch forms in the subtidal, intertidal or supratidal is controlled by several factors such as currents, wave action, slope angle, substrate and sediment supply. According to Kershaw and Guo (2001) abrasion notches can form as high as 2 m above msl as long as they are located on a coastline, which is exposed to the open ocean. However, Sur Lagoon nowadays is a very sheltered environment with a narrow entry and the available sediment within the lagoon is fine sand and mud, both ineffective abrading agents. Sur Lagoon is thereby not a suitable environment for the formation of abrasion notches nowadays, which is why we interpret the paleo abrasion notches as remains of a higher sea-level. Considering that Sur Lagoon is bordered by a Holocene barrier spit, which rarely exceeds a topographic elevation of 5 m above msl, even a small rise in sea-level will alter the shape of the lagoon significantly, potentially broaden the entry to the lagoon or even add additional entries.

Trenhaile (2015) clearly shows a correlation of notch width and exposure to waves or currents, leading to less wide notches in more sheltered positions. In Sur Lagoon we observe different notch widths in notches, which formed in the same substrate. The abrasion notches at outcrop E1, J1 and J2 all formed in sandy beachrock and show a width difference of 0.52 m, with E1 being 1.86 m wide and J1 and J2 being 1.35 m wide (see **Table 1** and **Figure 4**). The two abrasion notches that formed in fanglomerate substrate (E2 and F1) show only a width difference of 0.15 m with E2 being 1.86 m wide and F1 being 1.71 m wide. The differences in notch width do not match what would be expected based on their geographic position. The fact that the abrasion notches closer to the south of the lagoon (J1 and J2) are smaller and less well developed in comparison to the abrasion notch on the northern peninsula (E1) indicate a decline in wave-action towards the south, while in the modern setting of the lagoon the opposite is true. Notch E1 is located at the most sheltered position, further away from the entrance of lagoon, facing landwards.

The abrasion notches in fanglomerates (F1 and E2) are roughly of similar width also contradicting what would be expected from their geographic position. F1 is located directly at the entrance of the lagoon and thereby exposed to tidal currents and waves from the open ocean, while E2 is located on a peninsula inside Sur Lagoon, hence sheltered from strong waves. This further indicates a higher sea-level along with a different morphology of the lagoon at the time of notch formation. Furthermore, the symmetry of abrasion notches is influenced by their exposure to breaking waves. If waves are already broken, more symmetric shapes are formed (Sisma-Ventura et al. 2017). The notches at outcrops F1 and E1 are less symmetric than the notches at outcrops E2, J1 and J2 (see **Figure 4**), which indicates that these parts of the coastline were more often exposed to breaking waves, hence closer to the entry of the lagoon. Again pointing towards a possible second opening on the northwestern end of the lagoon during notch formation.

The abrasion notches in Sur Lagoon all occur between 1 to 3 m amsl with the exception of notch E2, whose floor is located 0.43 m lower. A similar height can indicate a similar age of formation and we observed no spatial relationship between the notches and other geological landmarks that oppose a similar age, but to confirm this more research, i.e. dating of the beachrocks at outcrops J and E1, is needed. As mentioned before, abrasion notches cannot be easily linked to a certain tidal datum (Pirazzoli 1986). However, some researchers have found that notch apex and high tide often coincide in recent abrasion notches along meso- and macro-tidal seas (Bini et al. 2014 and references therein). Investigating the present conditions of the study area like the tidal- and wave-regime as well as the availability of abrasive tools allows to draw conclusions on the relation between sea-level and the formation of abrasion notches (Bini et al. 2014). From these investigations we have already concluded that sea-level inside Sur Lagoon must have been higher during the formation of the abrasion notches and a different morphology of the lagoon is very likely. The question of how much higher

exactly remains subject of further studies, however the fact that the surfaces of these notches show no sign of bioerosion hints towards a position in the intertidal rather than permanently submerged. The apex being positioned at high tide is a plausible scenario. Barrier spits are generally very dynamic systems, that can change within the course of a severe storm or similar extreme wave event. A short term alteration of the shape of the lagoon can significantly heighten the tidal range within the lagoon by creating a larger connection to the open ocean.

### 5.3 Polyphase formation of the Bioerosion Notch

The formation of a bioerosion horizon is strictly tied to the tidal range, since the organisms responsible for the erosion live in a certain water depth. Together with a tidal notch, whose apex marks the position of msl during the formation of the notch, bioerosion is regarded to be a very precise indicator of past sea-level (Kelsey 2015).

Three phases of sea-level fluctuations can be recognized based on the bioerosion notches (Figure 9). The first phase implies an initial sea-level 3.93 m above msl, which is marked by the apex position (see Table 1, Kelsey 2015). This phase represents the formation of the bioerosion notch during stable sea-level conditions (Kelsey 2015).

*Lithophaga* was limited to the lower half of the notch with the apex as their upper limit (Laborel & Laborel-Deguen 1994, Rovere et al. 2015). The boring sponge *Cliona* was possibly present as well. The fossil traces of this boring sponge reaches up to the lower half of the notch and do not exceed the apex. However, shallow borings like *Cliona*, much like etchings and grazings, are often obliterated by *Lithophaga* and other deeper borings or abrasion and therefore hold a low preservation potential (see Bromley & Asgaard 1993).

We observe a second sea-level rise that did not last long enough to produce a notch shape of its own, but lead to colonization of the notch roof and beyond by *Lithophaga*. Coinciding with the edge of the notch roof *Lithophaga* borings occur very densely and form a distinct band at  $4.27 \text{ m} \pm 0.04 \text{ m}$  (amsl). Occasionally *Lithophaga* occur up to  $10.5 \text{ cm} \pm 6.8 \text{ cm}$  above the notch roof. The style of appearance above the notch roof is spotty and does not form a distinct line. While some authors argue that only a distinctive band like this is a precise sea-level indicator (Evelpidou et al. 2012b, Laborel & Laborel-Deguen 1994), others state that any *Lithophaga* boring shows a minimum limit for sea-level, because *Lithophaga* are primarily encountered several decimeters below msl (Rovere et

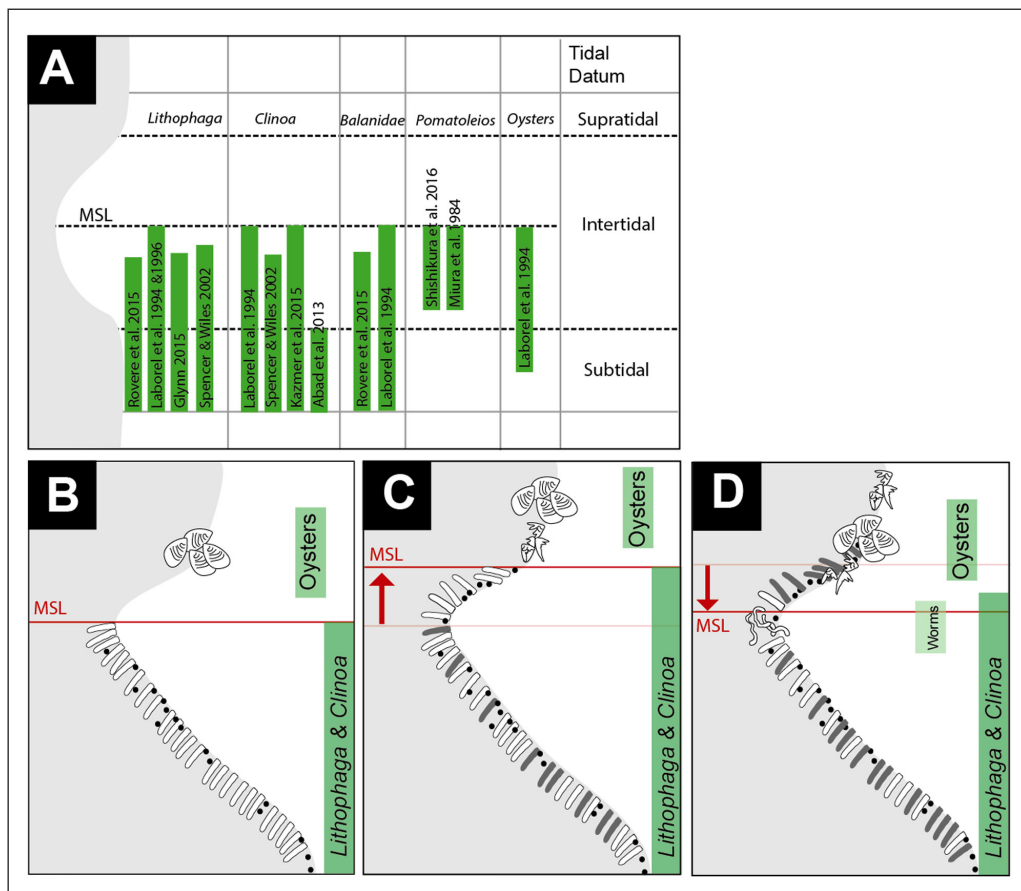


**Figure 9:** **A)** Position of organisms relative to MSL according to several publications. **B)** Formation of the notch. Msl is stable for a long time. *Lithophaga* are the most prominent bioeroders and reach up to the middle of the notch (apex). **C)** Oysters cover the eroded *Lithophaga* boreholes at the notch roof and occur above indicating a rising sea level. *Lithophaga* boreholes appear above the notch roof as well and support the theory of an increasing sea-level (Phase 2). In some cases *Lithophaga* bore through oyster shells. **D)** Msl drops. Barnacles and worm tubes occur inside of the notch and are present inside of *Lithophaga* boreholes as well as on the rock surface (Phase 3).

al. 2015, Vacchi et al. 2012). We conclude that msl must have risen at least 0.44 m in comparison to its level during notch formation to an elevation of 4.37 m. That this highstand did not produce a notch on its own and the distribution of *Lithophaga* borings is rather scarce suggests that the highstand was shorter than the one leading to notch formation. If sea-level rose directly from 3.93 m or if both highstands are interrupted by a regression cannot be stated at this point.

Oyster shells are present maximal 0.55 m above the roof of the notch. Investigations on recent oysters in the area show that they tend to cluster near the highest point of the tide. Based on this observation the oyster clusters at 4.82 m amsl possibly mark the paleo mean high water. Since the roof of bioerosion notches correlates with high tide, the oyster band above the roof also shows that sea-level rose higher than during notch formation.

*Pomatoleios kraussii* as well as *Balanidae* are covering and filling up *Lithophaga* boreholes inside of the bioerosion notch close to the apex. Both are known to settle in close proximity to msl (Rovere et al. 2015, Laborel et al. 1994, Shishikura et al. 2007). It is unlikely that these animals settled down during the initial phase of notch formation, as the fragile shells and tubes would most likely not withstand a prolonged submergence. This means they either settled down during the final regression or sea-level stabilized around 3.93 m again, after rising to 4.37 m. Again, a sea-level fall and subsequent transgression can also not be excluded.

The sequence ends with the filling of the notch with sandy beachrock, that we observe inside the notch, shortly below the apex, at outcrop A (see **Figure 8**). The beachrock succession at outcrop A represents a lower foreshore facies overlain by an upper foreshore facies, hence indicating deposition during regression. This beachrock shows that the upper limit of the upper foreshore, so mean high water, was shortly below the notch apex again 80 ka ago.

## 6 Conclusions

The main objectives of this study were to document the paleo coastal notches in the area of Sur Lagoon, to interpret them regarding their use as sea-level indicator and to test the hypothesis that the bioerosion notches represent a MIS 5e shoreline.

Three main conclusions can be summarised from the results:

1. The observed paleo shoreline in Sur Lagoon formed during the last interglacial MIS 5e. From the stratigraphical relationship of the notch to a beachrock and a fanglomerate, it becomes clear that notch-formation must have taken place between the deposition of the fanglomerate and the beachrock. The beachrock was previously dated to an age of 80 ka (Mauz et al. 2015) and the fanglomerate was dated in this study to a maximum age of 370 ka.
2. The coastal notches in Sur Lagoon fall into three categories: paleo notches with traces of bioero-

sion, paleo notches without traces of bioerosion and recent tidal notches whose formation is still ongoing. While the latter are obviously not indicative of paleo sea-level and the notches without bioerosion are challenging to tie to a certain tidal datum, the bioerosion notches constitute an excellent sea-level indicator. The shape and ichnofacies of these notches are very well preserved and the apex still lies horizontal and at the same height of  $3.93 \pm 0.12$  m at several outcrops around Sur Lagoon. This is indicative of the tectonic stability of the shoreline-section since notch formation, which coincides with results from previous studies of the area (Kusky et al. 2005; Ermertz et al. 2019; Hoffmann et al. 2020). It was concluded that sea-level during notch formation was  $3.93 \pm 0.12$  m higher than nowadays.

3. The organism distribution within the bioerosion notches documents at least one short-term sea-level fluctuation during the longer highstand, as the bioerosion traces show that msl temporarily rose to levels above the notch roof.

In summary, this study provides the first field-evidence of last interglacial shorelines on the coastline of Oman. In terms of sea-level research the Omani coastline is poorly studied and sea-level index points are missing from the entire area. Our results function as the basis for future investigations, which should focus on the establishment of sea-level index points and the detection of further outcrops that represent last interglacial shorelines in Oman. The short-term sea-level fluctuations during MIS 5e, that are documented in the bioerosion notches, also deserve further attention regarding a higher-resolution age constraint.

## Data Accessibility Statements

Datasets related to this article can be found at doi: 10.17632/symmbsbh2c.2 an open-source online data repository hosted at Mendeley Data (Falkenroth et al. 2019a).

## Acknowledgements

This paper is a contribution to IGCP Project 639 whose participants receive our thanks for fruitful discussions during a field trip to the study area in the scope of the 2016 meeting in Oman. Financial support by The Research Council Oman [TRC-grant ORG GUtech EBR 10 013; ORG-EBR-10-006] is gratefully acknowledged. The study was also funded by the Deutsche Forschungsgemeinschaft (DFG, German Research Foundation) with grant number [HO 2550/11-1]. Furthermore, this paper is part of the phd-project "Beachrock as Sea-Level Indicator", which receives funding by the Graduiertenförderung of the RWTH Aachen in form of a scholarship. Additionally, we express our gratitude to the GUtech in Muscat and the Rhenish Friedrich Wilhelm University in Bonn and their scientific staff who contributed the facilities and logistics that enabled this work. We further wish to thank Professor Simon

Engelhart in his function as editor at Open Quaternary and our reviewers, Matteo Vacchi and one anonymous, whose helpful remarks contributed to this manuscript.

#### Competing Interests

The authors have no competing interests to declare.

#### References

- Abad, M, Rodríguez-Vidal, J, Aboumaria, K, Zaghoul, MN, Cáceres, LM, Ruiz, F, Martínez-Aguirre, A, Izquierdo, T and Chamorro, S.** 2013. Evidence of MIS 5 sea-level highstands in Gebel Mousa coast (Strait of Gibraltar, North Africa). *Geomorphology*, 182: 133–146. DOI: <https://doi.org/10.1016/j.geomorph.2012.11.004>
- Al-Charaabi, Y and Al-Yahyai, S.** 2013. Projection of Future Changes in Rainfall and Temperature Patterns in Oman. *Journal of Earth Science and Climate Change*, 4: 154–161. DOI: <https://doi.org/10.4172/2157-7617.1000154>
- Antonioli, F, Lo Presti, V, Rovere, A, Ferranti, L, Anzidei, M, Furlani, S, Mastronuzzi, G, Orru, PE, Scicchitano, G, Sannino, G, Spampinato, CR, Pagliarulo, R, Deiana, G, de Sabata, E, Sansò, P, Vacchi, M and Vecchio, A.** 2015. Tidal notches in the Mediterranean Sea: a comprehensive analysis. *Quaternary Science Reviews*, 119: 66–84. DOI: <https://doi.org/10.1016/j.quascirev.2015.03.016>
- Balco, G, Stone, JO, Lifton, NA and Dunai, TJ.** 2008. A complete and easily accessible means of calculating surface exposure ages or erosion rates from  $^{10}\text{Be}$  and  $^{26}\text{Al}$  measurements. *Quaternary Geochronology*, 3: 174–195. DOI: <https://doi.org/10.1016/j.quageo.2007.12.001>
- Belal, AAM and Ghobashy, AFA.** 2012. Settlement behaviour and description of the lessepsian immigrant of the serpulid polychaete *Pomatoleios kraussii* in the Suez Bay. *Egyptian Journal of Aquatic Research*, 38: 23–30. DOI: <https://doi.org/10.1016/j.ejar.2012.09.001>
- Bini, M, Isola, I, Pappalardo, M, Ribolini, A, Favalli, M, Ragaini, L and Zanchetta, G.** 2014. Abrasion notches along the Atlantic Patagonian coast and their potential use as sea level markers: the case of Puerto Deseado (Santa Cruz, Argentina). *Earth Surface Processes and Landforms*, 39(11): 1550–1558. DOI: <https://doi.org/10.1002/esp.3612>
- Bintanja, R, Roderik, SW and van de Wal, OJ.** 2005. Modeled atmospheric temperatures and global sea levels over the past million years. *Nature*, 437: 125–128. DOI: <https://doi.org/10.1038/nature03975>
- Bromley, RG and Asgaard, U.** 1993. Two bioerosion ichnofacies produced by early and late burial associated with sea-level change. *Geologische Rundschau*, 82: 276–280. DOI: <https://doi.org/10.1007/BF00191833>
- Chesalin, MV, Al-Ghassani, SA and Balkhair, MA.** 2012. Species Identification of Rock Oysters Collected from the Dhofar Region, Sultanate of Oman. *Agricultural and Marine Sciences*, 17: 61–66. DOI: <https://doi.org/10.24200/jams.vol17iss0pp61-66>
- Dewald, A, Heinze, S, Jolie, J, Zilges, A, Dunai, TJ, Rethemeyer, J, Melles, M, Staubwasser, M, Kuczewski, B and Richter, J.** 2013. CologneAMS, a dedicated centre for accelerator mass spectrometry in Germany. *Nuclear Instruments and Methods in Physics Research Section B: Beam Interactions with Materials and Atoms*, 294: 18–23. DOI: <https://doi.org/10.1016/j.nimb.2012.04.030>
- Donato, SV, Reinhardt, EG, Boyce, JI, Pilarczyk, JE and Jupp, BP.** 2009. Particle-size distribution of inferred tsunami deposits in Sur Lagoon, Sultanate of Oman. *Marine Geology*, 257: 54–64. DOI: <https://doi.org/10.1016/j.margeo.2008.10.012>
- Ermertz, AM, Kázmér, M, Schneider, B, Adolphs, SK, Falkenroth, M and Hoffmann, G.** 2019. Active tectonics of the Arabian passive continental margin in Oman. *Open Quaternary*, 5: 1–14. DOI: <https://doi.org/10.5334/oq.56>
- Evelpidou, N, Kampolis, I, Pirazzoli, PA and Vassilopoulos, A.** 2012a. Global sea level rise and the disappearance of tidal notches. *Global and Planetary Change*, 92–93: 248–256. DOI: <https://doi.org/10.1016/j.gloplacha.2012.05.013>
- Evelpidou, N, Vassilopoulos, A and Pirazzoli, PA.** 2012b. Holocene emergence in Euboea island (Greece). *Marine Geology*, 295: 14–19. DOI: <https://doi.org/10.1016/j.margeo.2011.11.010>
- Falkenroth, M, Adolphs, S, Cahnbley, M, Bagci, H, Kazmer, M, Hoffmann, G and Mechernich, S.** 2019a. Coastal Notches in Sur (Sultanate of Oman) Dataset, Mendeley Data, V2.
- Falkenroth, M, Schneider, B and Hoffmann, G.** 2019b. Beachrock as sea-level indicator – A case study along the northeastern coastline of Oman (Indian Ocean). *Quaternary Science Reviews*, 206: 81–98. DOI: <https://doi.org/10.1016/j.quascirev.2019.01.003>
- Fournier, M, Léprier, C, Razin, P and Jolivet, L.** 2006. Late Cretaceous to Paleogene Post-obduction extension and subsequent Neogene compression in Oman Mountains. *Georabia*, 11(4): 17–40.
- Hearty, PJ, Hollin, JT, Neumann, AC and O’Leary, MJ.** 2007. Global sea-level fluctuations during the Last Interglaciation (MIS 5e). *Quaternary Science Reviews*, 26: 2090–2112. DOI: <https://doi.org/10.1016/j.quascirev.2007.06.019>
- Hearty, PJ and Tormey, BR.** 2017. Sea-level change and superstorms; geologic evidence from the last interglacial (MIS 5e) in the Bahamas and Bermuda offers ominous prospects for a warming Earth. *Marine Geology*, 390: 347–365. DOI: <https://doi.org/10.1016/j.margeo.2017.05.009>
- Hoffmann, G, Schneider, B, Mechernich, S, Falkenroth, M, Ermertz, A, Dunai, T and Preusser, F.** 2020. Quaternary uplift along a passive continental margin (Oman, Indian Ocean). *Geomorphology*, 350: 106870. DOI: <https://doi.org/10.1016/j.geomorph.2019.106870>

- IPCC, Allen, MR, Dube, OP, Solecki, W, Aragón-Durand, F, Cramer, W, Humphreys, S, Kainuma, M, Kala, J, Mahowald, N, Mulugetta, Y, Perez, R, Wairiu, M and Zickfeld, K.** 2018. Framing and Context. In: Masson-Delmotte, V, Zhai, P, Pörtner, H-O, Roberts, D, Skea, J, Shukla, PR, Pirani, A, Moufouma-Okia, W, Péan, C, Pidcock, R, Connors, S, Matthews, JBR, Chen, Y, Zhou, X, Gomis, MI, Lonnoy, E, Maycock, T, Tignor, M and Waterfield, T (eds.), *Global Warming of 1.5°C*. An IPCC Special Report on the impacts of global warming of 1.5°C above pre-industrial levels and related global greenhouse gas emission pathways, in the context of strengthening the global response to the threat of climate change, sustainable development, and efforts to eradicate poverty. In Press.
- IPCC, Stocker, TF, Quin, D, Plattner, GK, Tignor, M, Allen, SK, Boschung, J, Nauels, A, Xia, Y, Bex, V, and Midgley, PM.** 2013. Climate Change 2013. The Physical Science Basis. Working Group I Contribution to the Fifth Assessment Report of the Intergovernmental Panel on Climate Change-Abstract for Decision-Makers.
- Kázmér, M, Leman, MS, Mohamed, KR, Ali, CA and Taboroši, D.** 2015. Features of Intertidal Bioerosion and Bioconstruction on Limestone Coasts of Langkawi Islands, Malaysia. *Sains Malaysiana*, 44: 921–929. DOI: <https://doi.org/10.17576/jsm-2015-4407-02>
- Kázmér, M and Taboroši, D.** 2012. Rapid Profiling of Marine Notches Using a Handheld Laser Distance Meter. *Journal of Coastal Research*, 28(4): 964–969. DOI: <https://doi.org/10.2112/JCOASTRES-D-11-00163.1>
- Kelsey, H.** 2015. Geomorphological indicators of past sea levels. In: Shennan, I, Long, AJ and Horton, BP (eds.), *Handbook of Sea-Level Research*, 66–82. Chichester, UK: Wiley. DOI: <https://doi.org/10.1002/9781118452547.ch5>
- Kershaw, S and Guo, L.** 2001. Marine notches in coastal cliffs: indicators of relative sea-level change, Perachora Peninsula, central Greece. *Marine Geology*, 179: 213–228. DOI: [https://doi.org/10.1016/S0025-3227\(01\)00218-3](https://doi.org/10.1016/S0025-3227(01)00218-3)
- Kline, SW, Adams, PN and Limber, PW.** 2014. The unsteady nature of sea cliff retreat due to mechanical abrasion, failure and comminution feedbacks. *Geomorphology*, 219: 53–67. DOI: <https://doi.org/10.1016/j.geomorph.2014.03.037>
- Kopp, RE, Simons, FJ, Mitrovica, JX, Maloof, AC and Oppenheimer, M.** 2009. Probabilistic assessment of sea-level during the last interglacial stage. *Nature*, 462: 863–867. DOI: <https://doi.org/10.1038/nature08686>
- Kusky, T, Robinson, C and El-Baz, F.** 2005. Tertiary-Quaternary faulting and uplift in the northern Oman Hajar Mountains. *Journal of the Geological Society*, 162(5): 871–888. DOI: <https://doi.org/10.1144/0016-764904-122>
- Kwarteng, AY, Dorvlo, AS and Vijaya Kumar, GT.** 2009. Analysis of a 27-year rainfall data (1977–2003) in the Sultanate of Oman. *International Journal of Climatology*, 29: 605–617. DOI: <https://doi.org/10.1002/joc.1727>
- Laborel, J and Laborel-Deguen, F.** 1994. Biological Indicators of Relative Sea-Level Variations and of Co-Seismic Displacements in the Mediterranean Region. *Journal of Coastal Research*, 10(2): 395–415.
- Laborel, J, Morhange, C, Lafont, R, Le Champion, J, Laborel-Deguen, F and Sartoreto, S.** 1994. Biological evidence of sea-level rise during the last 4500 years on the rocky coasts of continental southwestern France and Corsica. *Marine Geology*, 120(3–4): 203–223. DOI: [https://doi.org/10.1016/0025-3227\(94\)90059-0](https://doi.org/10.1016/0025-3227(94)90059-0)
- Lifton, N, Sato, T and Dunai, TJ.** 2014. Scaling in situ cosmogenic nuclide production rates using analytical approximations to atmospheric cosmic-ray fluxes. *Earth Planetary Science Letters*, 386: 149–160. DOI: <https://doi.org/10.1016/j.epsl.2013.10.052>
- Lorscheid, T, Stocchi, P, Casella, E, Gómez-Pujol, L, Vacchi, M, Mann, T and Rovere, A.** 2017. Paleo sea-level changes and relative sea-level indicators: Precise measurements, indicative meaning and glacial isostatic adjustment perspectives from Mallorca (Western Mediterranean). *Paleogeography, Paleoclimatology, Paleoecology*, 473: 94–107. DOI: <https://doi.org/10.1016/j.palaeo.2017.02.028>
- Lüthi, D, Le Floch, M, Bereiter, B, Blunier, T, Barnola, JM, Siegenthaler, U, Raynaud, D, Jouzel, J, Fischer, H, Kawamura, K and Stocker, TF.** 2008. High-resolution carbon dioxide concentration record 650,000–800,000 years before present. *Nature*, 453(7193): 379. DOI: <https://doi.org/10.1038/nature06949>
- Mauz, B, Vacchi, M, Green, A, Hoffmann, G and Cooper, A.** 2015. Beach rock: A tool for reconstructing relative sea level in the far-field. *Marine Geology*, 362: 1–16. DOI: <https://doi.org/10.1016/j.margeo.2015.01.009>
- McLachlan, A, Fisher, HN, Al-Habsi, S, Al-Shukairi, SS and Al-Habsi, AM.** 1998. Ecology of sandy beaches in Oman. *Journal of Coastal Conservation*, 4: 181–190. DOI: <https://doi.org/10.1007/BF02806510>
- Miller, W.** 2007. *Trace fossils – Concepts Problems Prospects*, 611. Amsterdam: Elsevier.
- Nava, H and Carballo, JL.** 2008. Chemical and mechanical bioerosion of boring sponges from Mexican Pacific coral reefs. *Journal of experimental Biology*, 211(17): 2827–2831. DOI: <https://doi.org/10.1242/jeb.019216>
- Nishiizumi, K, Imamura, M, Caffee, MW, Southon, JR, Finkel, RC and McAninch, J.** 2007. Absolute calibration of <sup>10</sup>Be AMS standards. *Nuclear Instruments and Methods in Physics Research Section B: Beam Interactions with Materials and Atoms*, 258: 403–413. DOI: <https://doi.org/10.1016/j.nimb.2007.01.297>
- Otto-Bliesner, BL, Marshall, SJ, Overpeck, JT, Miller, GH and Hu, A.** 2006. Simulating Arctic climate warmth and icefield retreat in the last interglaciation. *Science*, 311: 1751–1753. DOI: <https://doi.org/10.1126/science.1120808>

- Pérés, JM.** 1982. Zonations and organismic assemblages. In: Kinne, O (ed.), *Marine Ecology*, 9–576. John Wiley & Sons, Chichester.
- Petit, JR, Jouzel, J, Raynaud, D, Barkov, NI, Barnola, JM, Basile, I, Bender, M, Chappellaz, J, Davis, M, and Delaygue, G.** 1999. Climate and atmospheric history of the past 420,000 years from the Vostok ice core, Antarctica. *Nature*, 399: 429–436. DOI: <https://doi.org/10.1038/20859>
- Pirazzoli, PA.** 1986. Marine notches. In Van De Plassche, O (ed.), *Sea-Level Research*, 361–400. Springer, Netherlands. DOI: [https://doi.org/10.1007/978-94-009-4215-8\\_12](https://doi.org/10.1007/978-94-009-4215-8_12)
- Rohling, EJ, Grant, K, Hemleben, CH, Siddall, M, Hoogakker, BAA, Bolshaw, M and Kucera, M.** 2008. High rates of sea-level rise during the last interglacial period. *Nature Geoscience*, 1(1): 38. DOI: <https://doi.org/10.1038/ngeo.2007.28>
- Rovere, A, Antonioli, F and Bianchi, CN.** 2015. Fixed Biological indicators. In Shennan, I, Long, AJ and Horton, BP (eds.), *Handbook of Sea-Level Research*, Chichester, 268–280. UK: Wiley. DOI: <https://doi.org/10.1002/9781118452547.ch18>
- Rovere, A, Raymo, ME, Vacchi, M, Lorscheid, T, Stocchi, P, Gómez-Pujol, L, Harris, DL, Casella, E, O’Leary, MJ and Hearty, PJ.** 2016. The analysis of Last Interglacial (MIS 5e) relative sea-level indicators: Reconstructing sea-level in a warmer world. *Earth-Science Reviews*, 159: 404–427. DOI: <https://doi.org/10.1016/j.earscirev.2016.06.006>
- Rust, D and Kershaw, S.** 2000. Holocene tectonic uplift patterns in northeastern Sicily: evidence from marine notches in coastal outcrops. *Marine Geology*, 167: 105–126. DOI: [https://doi.org/10.1016/S0025-3227\(00\)00019-0](https://doi.org/10.1016/S0025-3227(00)00019-0)
- Schmidt, S, Hetzel, R, Kuhlmann, J, Mingorance, F and Ramos, VA.** 2011. A note of caution on the use of boulders for exposure dating of depositional surfaces. *Earth and Planetary Science Letters*, 302: 60–70. DOI: <https://doi.org/10.1016/j.epsl.2010.11.039>
- Schneiderwind, S, Kázmér, M, Boulton, S, Papanikolaou, I and Reicherter, K.** 2016. Geometry of Holocene tidal notches – sea level markers at Perachora peninsula, Gulf of Corinth, Greece. *Bulletin of the Geological Society of Greece*, 50(1): 468–477. DOI: <https://doi.org/10.12681/bgsg.11748>
- Shackleton, NJ, Sánchez-Göni, MF, Pailler, D and Lancelot, Y.** 2003. Marine Isotope Substage 5e and the Eemian Interglacial. *Global and Planetary Change*, 36: 151–155. DOI: [https://doi.org/10.1016/S0921-8181\(02\)00181-9](https://doi.org/10.1016/S0921-8181(02)00181-9)
- Shalla, SH and Holt, TJ.** 1999. The Lessepsian migrant *Pomatoleios kraussii* (Annelida, Polychaeta) – recent formation of dense aggregations in Lake Timsah and the Bitter Lakes (Suez Canal, Egypt). *Egyptian Journal of Biology*, 1: 133–137.
- Shishikura, M, Echigo, T and Kaneda, H.** 2007. Marine reservoir correction for the Pacific coast of central Japan using <sup>14</sup>C ages of marine mollusks uplifted during historical earthquakes. *Quaternary Research*, 67(2): 286–291. DOI: <https://doi.org/10.1016/j.yqres.2006.09.003>
- Sidall, M, Chappell, J and Potter, EK.** 2006. Eustatic Sea Level During Past Interglacials, In: Sirocko, F, Litt, T, Claussen, M and Sanchez-Goni, MF (eds.), *The climate of past interglacials*. Elsevier, Amsterdam. DOI: [https://doi.org/10.1016/S1571-0866\(07\)80032-7](https://doi.org/10.1016/S1571-0866(07)80032-7)
- Sisma-Ventura, G, Sivan, D, Shtienberg, G, Bialik, OM, Filin, S and Greenbaum, N.** 2017. Last interglacial sea level high-stand deduced from well-preserved abrasive notches exposed on the Galilee coast of northern Israel. *Palaeogeography, Palaeoclimatology, Palaeoecology*, 470: 1–10. DOI: <https://doi.org/10.1016/j.palaeo.2017.01.008>
- Stirling, CH, Esat, TM, Lambeck, K and McCulloch, MT.** 1998. Timing and duration of the Last Interglacial: evidence for a restricted interval of widespread coral reef growth. *Earth and Planetary Science Letters*, 160: 18. DOI: [https://doi.org/10.1016/S0012-821X\(98\)00125-3](https://doi.org/10.1016/S0012-821X(98)00125-3)
- Stone, JO.** 2000. Air pressure and cosmogenic isotope production. *Journal of Geophysical Research on Solid Earth*, 105(B10): 23753–23756. DOI: <https://doi.org/10.1029/2000JB900181>
- Straughan, D.** 1969. Intertidal Zone-Formation in *Pomatoleios kraussii* (Annelida: Polychaeta). *Biological Bulletin*, 136(6): 469–482. DOI: <https://doi.org/10.2307/1539689>
- Trenhaile, AS.** 2015. Coastal notches: Their morphology, formation, and function. *Earth-Science Reviews*, 150: 285–304. DOI: <https://doi.org/10.1016/j.earscirev.2015.08.003>
- Vacchi, M, Rovere, A, Zouros, N, Desruelles, S, Caron, V and Firpo, M.** 2012. Spatial distribution of sea-level markers on Lesbos Island (NE Aegean Sea): evidence of differential relative sea-level changes and the neotectonic implications. *Geomorphology*, 159: 50–62. DOI: <https://doi.org/10.1016/j.geomorph.2012.03.004>
- Westerheide, W and Rieger, R.** 2007. *Spezielle Zoologie – Teil 1: Einzeller und Wirbellose Tiere*. Elsevier, Spektrum Akademischer Verlag, München, 976.
- Wyns, R, Le Métour, J, Roger, J and Chevrel, S.** 1992. Geological Map of Sur 1:250,000, Sheet NF 40–08, explanatory notes. Ministry of petroleum and Minerals, Directorate General of Minerals, Muscat, Oman, 80.

**How to cite this article:** Falkenroth, M, Adolphs, S, Cahnbley, M, Bagci, H, Kázmér, M, Mechernich, S and Hoffmann, G. 2020. Biological Indicators Reveal Small-Scale Sea-Level Variability During MIS 5e (Sur, Sultanate of Oman). *Open Quaternary*, 6: 1, pp. 1–20. DOI: <https://doi.org/10.5334/oq.72>

**Submitted:** 19 August 2019

**Accepted:** 13 December 2019

**Published:** 13 January 2020

**Copyright:** © 2020 The Author(s). This is an open-access article distributed under the terms of the Creative Commons Attribution 4.0 International License (CC-BY 4.0), which permits unrestricted use, distribution, and reproduction in any medium, provided the original author and source are credited. See <http://creativecommons.org/licenses/by/4.0/>.

 *Open Quaternary* is a peer-reviewed open access journal published by Ubiquity Press.

**OPEN ACCESS** 